

SCATTERING OF ^{15}N IONS BY $^{10,11}\text{B}$ NUCLEI
AT THE ENERGY OF 43 MeV*

N. BURTEBAYEV^a, N. AMANGELDI^{a,b}, D. ALIMOV^a, ZH. KERIMKULOV^a
B. MAUYEY^{a,b,i}, M. NASSURLLA^a, YE. KOK^{a,b}, S.B. SAKUTA^c
S.V. ARTEMOV^d, A.A. KARAKHODJAEV^d, K. RUSEK^e, E. PIASECKI^e
A. TRZCINSKA^e, M. WOLINSKA-CICHOCKA^e, I. BOSTOSUN^f
M. KARAKOC^f, SH. HAMADA^g, S.YU. TORILOV^h
B. ZALEWSKIⁱ, J.M. MUSSAEV^j

^aInstitute of Nuclear Physics, Almaty, Kazakhstan

^bL.N. Gumilyov Eurasian National University, Astana, Kazakhstan

^cNational Research Center “Kurchatov Institute”, Moscow, Russia

^dInstitute of Nuclear Physics, Academy of Sciences, Republic of Uzbekistan

^eHeavy Ion Laboratory, University of Warsaw, Warszawa, Poland

^fDepartment of Physics, Akdeniz University, Antalya, Turkey

^gFaculty of Science, Tanta University, Tanta, Egypt

^hSaint Petersburg State University, Saint Petersburg, Russia

ⁱJoint Institute of Nuclear Research, Dubna, JINR

^jSouth Kazakhstan State University, Shymkent, Kazakhstan

(Received December 28, 2017)

Angular distributions for ^{15}N elastically scattered from $^{10,11}\text{B}$ nuclei were measured at the energy of 43 MeV. The experimental data for the $^{11}\text{B}+^{15}\text{N}$ system showed a remarkable increase in differential cross sections at large angles which cannot be explained within the framework of the optical model. Such behavior of the cross sections can be reproduced only by taking into account the contribution of the α -cluster transfer mechanism. Although the experimental data for $^{10}\text{B}+^{15}\text{N}$ system showed an increase in differential cross sections at backward angles, it can be described by optical model calculations.

DOI:10.5506/APhysPolBSupp.11.99

1. Introduction

In the sixties, an unexpected result was obtained when studying the scattering of α -particles. The measured cross sections increased strongly in the region of large angles, whereas calculations based on nuclear potential

* Presented at the XXIV Nuclear Physics Workshop “Marie and Pierre Curie”, Kazimierz Dolny, Poland, September 20–24, 2017.

scattering predicted a decrease [1–3]. This effect was named Anomalous Large Angles Scattering (ALAS) leading to many experimental and theoretical efforts to explain it. This effect turned out to be highly-dependent on the structure of the target nucleus. These studies also showed that measurements at large angles could lead to significant new physics understanding. In this regard, the study of the elastic scattering and transfer reactions for heavier projectiles at energies close to the Coulomb barrier is very interesting. It is now known that when scattered particles have a pronounced cluster structure (for example, such as ${}^6\text{Li}$, ${}^7\text{Li}$, ${}^9\text{Be}$ and N -alpha nuclei (${}^{12}\text{C}$, ${}^{16}\text{O}$, ${}^{20}\text{N}$)), a distinct increase in the differential cross sections in the backward hemisphere is also observed. In calculations, this behavior can be reproduced by taking into account the contribution of nucleon or cluster of nucleons transfer between the projectile and the target nucleus. Recently, elastic scattering and α -cluster transfer between ${}^{15}\text{N}$ and ${}^{11}\text{B}$ at 84 MeV has been studied by Rudchik *et al.* [4] and a significant increase in the differential cross sections at backward angles was observed. It is known that the contribution of transfer reactions strongly depends on the structure of the two interacting nuclei, as well as on the beam energy. In this paper, we report the research results of elastic scattering for the systems ${}^{15}\text{N} + {}^{10,11}\text{B}$ at $E_{\text{lab}}({}^{15}\text{N}) = 43$ MeV to explore the scattering at forward and backward angles. Elastic scattering studies provide key information for understanding the cluster structure and the clusterization probability of nuclei. The main motivation of the present experimental angular distributions measurements was to examine the cluster structure of the ${}^{15}\text{N}$ nucleus. The two clusterization probabilities for ${}^{15}\text{N}$ which are explored in this work are: (a) ${}^{15}\text{N}$ as a clusterized nucleus consisting of a core (${}^{11}\text{B}$) plus a valence (${}^4\text{He}$) and (b) ${}^{15}\text{N}$ as a clusterized nucleus consisting of a core (${}^{10}\text{B}$) plus a valence (${}^5\text{He}$). Based on theoretical calculations, the first probability is highly likely and has a significant role in formation of the cross sections at backward angles. On the other hand, the second probability is small and should not give a large contribution. The present data showed a remarkable increase in differential cross sections at large angles for both ${}^{15}\text{N}+{}^{11}\text{B}$ and ${}^{15}\text{N}+{}^{10}\text{B}$ systems. This rise in differential cross sections at backward angles in ${}^{15}\text{N}+{}^{11}\text{B}$ system cannot be reproduced using the optical model (OM) alone but requires the inclusion of α -cluster transfer using the distorted waves Born approximation (DWBA) method. For the ${}^{15}\text{N}+{}^{10}\text{B}$ system, the theoretical OM calculations could fairly reproduce the data at forward and backward angles which gives evidence for the low clusterization probability for ${}^{15}\text{N}$ as a core (${}^{10}\text{B}$) plus a valence (${}^5\text{He}$). The large angle data then explore differences such as cluster probabilities and ground state quadrupole moments.

2. Experimental procedure and measurement results

The experiment was performed with the U-200P cyclotron at the Heavy Ion Laboratory, University of Warsaw. A beam of ^{15}N accelerated up to the energy of 43 MeV was focused on the target located in the center of the scattering chamber, which is the basis of the multi-detector system ICARE [5,6]. The target thicknesses of ^{10}B and ^{11}B were 0.15 mg/cm^2 and 0.25 mg/cm^2 , respectively. For the manufacture of these targets, we used the technique of vacuum evaporation by resistance heating of the specimen with a spot electron gun at the facility UKP-2 in the Institute of Nuclear Physics (Almaty, Kazakhstan). In our experiment, the detection system was equipped with four $(\Delta E-E)$ telescopes consisting of silicon detectors (E) about $300\text{ }\mu\text{m}$ in thickness and ionization chambers (ΔE) filled with isobutene (C_4H_{10}) to a pressure of 25 Torr. In addition, three silicon detectors located at an angle of 15° were used to monitor the beam and measure its energy. In the present measurements, standard CAMAC electronics and the data acquisition system MIDAS and SMAN [7] were used. This allowed us to identify charged particles up to $Z = 10$. The measured energy spectra were analyzed using the program ROOT [8]. A typical two-dimensional spectrum $(\Delta E-E)$ is shown in Fig. 1. Angular distributions of ^{15}N scattered by $^{10,11}\text{B}$ nuclei were measured in the angular range of 5° – 40° in the laboratory system. They are shown in Figs. 2–4 by black points. The differential cross sections of the scattered ^{15}N nuclei at angles greater than 100° were obtained by detecting the ^{10}B and ^{11}B recoil nuclei. As can be seen from the figures, the almost monotonic decrease in the cross sections in the region of the forward hemisphere is accompanied by its noticeable rise at large angles.

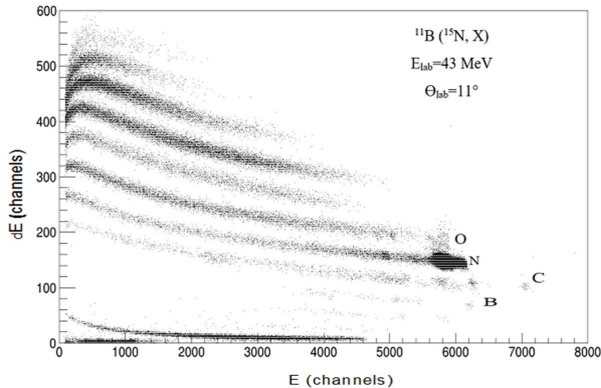


Fig. 1. Typical $\Delta E-E$ spectrum of the $^{11}\text{B}(^{15}\text{N}, X)$ reaction products at $E_{\text{lab}}(^{15}\text{N}) = 43\text{ MeV}$ measured at the angle $\theta_{\text{lab}} = 11^\circ$.

3. Analysis of experimental data and discussion

3.1. Elastic scattering

As a first step, the experimental data for the $^{15}\text{N}+^{11}\text{B}$ and $^{15}\text{N}+^{10}\text{B}$ nuclear systems were analyzed under the assumption of pure potential scattering. In this case, the differential cross sections were calculated in the framework of the OM. Two approaches were used. The first approach was phenomenological and the interaction potential was found by fitting the calculated cross sections to the experimental data. In this analysis, the optical potential (OP) was described by a Woods–Saxon form factor for both the real and imaginary parts of the nuclear potential (the last two terms in the following formula)

$$U(\mathbf{r}) = V_C(\mathbf{r}) - V_0 \left[1 + \exp\left(\frac{r - R_V}{a_V}\right) \right]^{-1} - iW_0 \left[1 + \exp\left(\frac{r - R_W}{a_W}\right) \right]^{-1}. \quad (1)$$

Here, V_0 , a_V and W_0 , a_W are the depths and diffusenesses of the real and imaginary parts of the nuclear potentials, respectively. V_C is the Coulomb potential of a uniform charged sphere, radii in these expressions are defined as $R_i = r_i (A_p^{1/3} + A_t^{1/3})$, $i = V, W, C$.

In the microscopic approach, a double folding optical potential (DFOP) which derives the real part of the potential using the double folding potential (DFP) procedure was used in addition to a Woods–Saxon imaginary volume potential. This approach folds the density distributions of the projectile and the target with the nucleon–nucleon interaction potential $V_{NN}(r)$. The nucleon–nucleon interaction was taken to be of the CDM3Y6 form based on the M3Y-Paris potential [9, 10]. The density distributions $\rho(r)$ of ^{10}B , ^{11}B , and ^{15}N were calculated using a Modified Harmonic Oscillator (MHO) [11]: $\rho(r) = \rho_0 [1 + \alpha(\frac{r}{a})^2] \exp[-(\frac{r}{a})^2]$, the parameters ρ_0 , a , α as well as the quadrupole moments for ^{10}B , ^{11}B and the root-mean-square radii of the charge distributions for ^{10}B , ^{11}B , and ^{15}N are listed in Table I.

TABLE I

Parameters of MHO used in calculating density distributions of ^{10}B , ^{11}B , and ^{15}N nuclei.

| Nucleus | ρ_0 | a | α | $\langle r^2 \rangle^{1/2}$ | $Q(\text{b})$ |
|-----------------|----------|------|----------|-----------------------------|---------------|
| ^{10}B | 0.1818 | 1.71 | 0.837 | 2.45 | 0.0847 |
| ^{11}B | 0.1818 | 1.69 | 0.811 | 2.42 | 0.0407 |
| ^{15}N | 0.158 | 1.81 | 1.25 | 2.65 | — |

The potential in this case has the following shape:

$$U(\mathbf{r}) = V_C(\mathbf{r}) - N_r V^{\text{DF}}(\mathbf{r}) - iW_0 \left[1 + \exp\left(\frac{r - R_W}{a_W}\right) \right]^{-1}, \quad (2)$$

here N_r is a renormalization factor. The double folding calculations were performed using the code DFMSPH [12].

The experimental angular distribution data for $^{11}\text{B}(^{15}\text{N}, ^{15}\text{N})^{11}\text{B}$ and $^{10}\text{B}(^{15}\text{N}, ^{15}\text{N})^{10}\text{B}$ at the energy $E_{\text{lab}}(^{15}\text{N}) = 43$ MeV were analyzed at angles up to 90° (forward hemisphere) to exclude the effect of cluster transfer which can produce significant features at large angles (backward hemisphere). Data at forward angles for pure elastic scattering were analyzed using both OP Eq. (1) and DFOP Eq. (2) with the FRESCO code [13]. The potential parameters extracted from the phenomenological and microscopic analyses are presented in Tables II and III. Our DFP for the two considered nuclear systems $^{15}\text{N}+^{11}\text{B}$ and $^{15}\text{N}+^{10}\text{B}$ do not require any renormalization ($N_r = 1$). The comparisons between the theoretical calculations and the experimental data for $^{11}\text{B}(^{15}\text{N}, ^{15}\text{N})^{11}\text{B}$ and $^{10}\text{B}(^{15}\text{N}, ^{15}\text{N})^{10}\text{B}$ are shown in Figs. 2–4.

TABLE II

Optimal OP and DFOP parameters for the $^{15}\text{N}+^{11}\text{B}$ nuclear system at $E_{\text{lab}}(^{15}\text{N}) = 43$ MeV, the Coulomb radius parameter was fixed at 1.25 fm.

| Model | Potential | V_0 | r_V | a_V | N_r | W_0 | r_W | a_W | SA |
|--------|-----------|-------|-------|-------|-------|-------|-------|-------|-------|
| OM OP | OP | 200 | 0.79 | 0.75 | — | 11.0 | 1.25 | 0.75 | — |
| DWBA | — | — | — | — | — | — | — | — | 0.435 |
| OM DFP | DFOP | — | — | — | 1 | 11.0 | 1.25 | 0.75 | — |
| DWBA | — | — | — | — | 1 | — | — | — | 0.435 |

TABLE III

The same as Table II but for $^{15}\text{N}+^{10}\text{B}$ nuclear system.

| Model | Potential | V_0 | r_V | a_V | N_r | W_0 | r_W | a_W |
|--------|-----------|-------|-------|-------|-------|-------|-------|-------|
| OM OP | OP | 205.7 | 0.79 | 0.831 | — | 8.48 | 1.25 | 0.95 |
| OM DFP | DFOP | — | — | — | 1 | 9.94 | 1.25 | 0.97 |

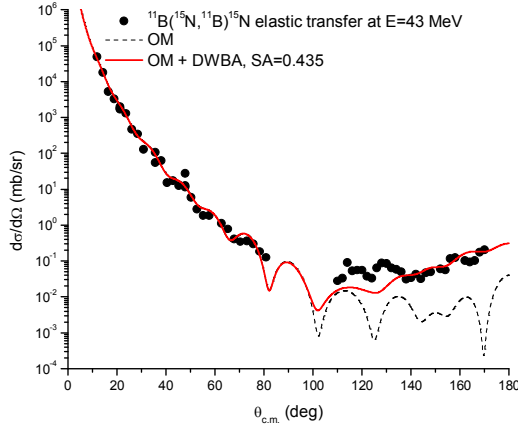


Fig. 2. Comparison between experimental data for the $^{15}\text{N}+^{11}\text{B}$ nuclear system (black points) and OM calculations for pure elastic scattering (dashed/black line) and DWBA for α -cluster transfer (solid/red line) using OP.

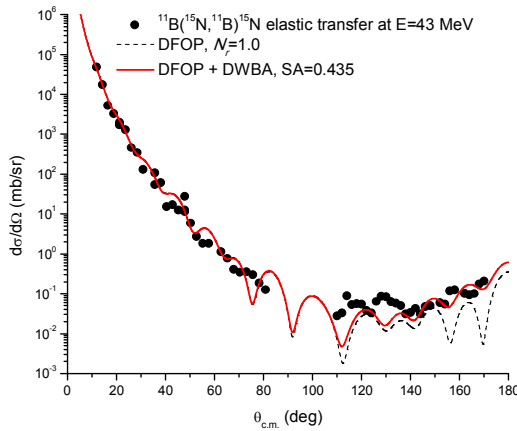


Fig. 3. The same as Fig. 2 but calculations were performed using DFOP.

3.2. Taking into account the cluster exchange effects

As mentioned earlier, the large differential cross sections at backward angles can be due to cluster transfer. DWBA calculations were performed to explore the possibility that ^{15}N can be treated as composed of $^{11}\text{B}+\alpha$. The diagram corresponding to this process is shown in Fig. 5. In this case, the exchange of an α -cluster between the interacting nuclei leads to an exit channel that is physically indistinguishable from the entrance channel. So, the situation in elastic scattering becomes more complicated and the differential cross section will be the square of the sum of amplitudes from the

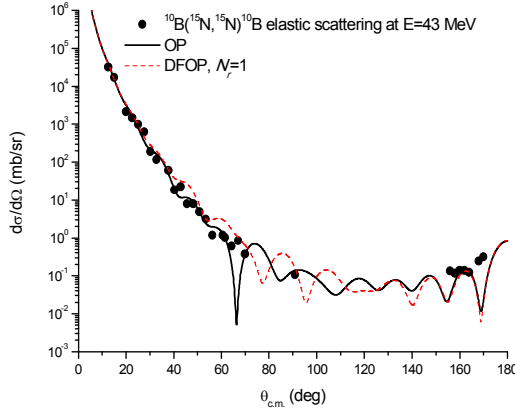


Fig. 4. Comparison between experimental data for $^{15}\text{N}+^{10}\text{B}$ nuclear system (black points) and theoretical OM calculations using OP (black line) and DFOP (dashed/red line).

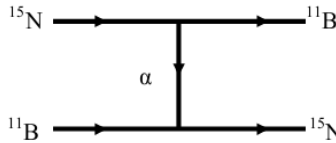


Fig. 5. Diagram of the α -cluster exchange mechanism in the scattering of ^{15}N by ^{11}B nuclei.

pure elastic scattering and the exchange mechanism of the cluster transfer as follows: $\frac{d\sigma_{\text{el}}}{d\Omega} = |f_{\text{el}}(\theta) + e^{i\alpha} S f_{\text{DWBA}}(\pi - \theta)|^2$, where $f_{\text{el}}(\theta)$ is the elastic scattering amplitude, $f_{\text{DWBA}}(\pi - \theta)$ is the amplitude calculated in the distorted wave method with the replacement $\theta \rightarrow \pi - \theta$, S is the product of the two spectroscopic amplitudes (SA) of the transferred particle in the initial and final states which, by the way, are the same in the case of elastic transfer. Within the framework of this model, the same OP parameters which reproduce well the experimental data in the forward hemisphere (pure elastic scattering) are usually used, and the spectroscopic amplitude is taken as a free parameter which is varied to give the best agreement between the theoretical calculations and the experimental data. The extracted SA for the configuration $^{15}\text{N} \rightarrow ^{11}\text{B} + \alpha$ is 0.435 which is in a good agreement with that reported in Ref. [4].

The bound state wave function for the relative motion of the α and ^{11}B in ^{15}N is defined by a Woods–Saxon potential with fixed radius $R = 1.25 \times (A_{\text{p}}^{1/3} + A_{\text{t}}^{1/3})$ fm and the diffuseness $a = 0.65$ fm. The potential depth was adjusted to reproduce the binding energy of the cluster. The

number of nodes (N) were determined using the Talmi–Moshinsky formula [14]: $2(N - 1) + L = \sum_{i=1}^n 2(n_i - 1) + l_i$, where n_i and l_i are quantum numbers of nucleons in the cluster; L is orbital momentum of the cluster. Cluster quantum numbers for the overlap used in our calculations are listed in Table IV.

TABLE IV

Cluster quantum numbers for the overlaps used in our calculations.

| Overlap | N | L | S | $J = L + S$ | B.E. [MeV] |
|--|-----|-----|-----|-------------|------------|
| $\langle {}^{15}\text{N} {}^{11}\text{B}\rangle$ | 2 | 2 | 0 | 2 | 10.991 |

4. Summary

We have measured elastic scattering angular distributions for the ${}^{15}\text{N}+{}^{11}\text{B}$ and ${}^{15}\text{N}+{}^{10}\text{B}$ systems at the energy of $E_{\text{lab}}({}^{15}\text{N}) = 43$ MeV. The experimental data for the ${}^{15}\text{N}+{}^{11}\text{B}$ nuclear system at backward angles showed a remarkable increase in differential cross section. These data were analyzed within the framework of the OM to reproduce the cross sections in the forward hemisphere (pure elastic scattering) and the DWBA method to reproduce the data in the backward hemisphere (elastic transfer). Both OM and DWBA calculations were performed using both OP — Woods–Saxon-type real and imaginary potentials — and DFP for the real part (with $N_r = 1$) plus the Woods–Saxon-type imaginary potential. These results show that the back angle cross section is a measure of the α -cluster transfer probability. On the other hand, the experimental data for the ${}^{15}\text{N}+{}^{10}\text{B}$ nuclear system are fairly well-reproduced using both the OP and DFOP over the whole angular range which shows that there is a low clustering probability of ${}^{15}\text{N}$ to be in the form as ${}^{10}\text{B}$ (core) + ${}^5\text{He}$ (valence).

This project has received funding from the European Union’s Horizon 2020 research and innovation programme under grant agreement No. 654002.

REFERENCES

- [1] A. Budzanowski *et al.*, *Phys. Lett.* **16**, 135 (1965).
- [2] A. Bobrowska *et al.*, *Nucl. Phys. A* **126**, 361 (1969).
- [3] C.R. Gruhn, N.S. Wall, *Nucl. Phys.* **81**, 161 (1966).
- [4] A.T. Rudchik *et al.*, *Nucl. Phys. A* **939**, 1 (2015).
- [5] M. Rousseau *et al.*, *Phys. Rev. C* **66**, 034612 (2002).

- [6] C. Bhattacharya *et al.*, *Phys. Rev. C* **65**, 014611 (2001).
- [7] M. Kowalczyk, SMAN: a code for nuclear experiments, Warszawa 1997, unpublished.
- [8] ROOT, A Data Analysis Framework, <http://root.cern.ch/drupal/>
- [9] G.R. Satchler, W.G. Love, *Phys. Rep.* **55**, 183 (1979).
- [10] D.T. Khoa, G.R. Satchler, W. Von Oertzen, *Phys. Rev. C* **56**, 954 (1997).
- [11] H. De Vries, C.W. De Jager, C. De Vries, *Atomic Data Nucl. Data Tables* **36**, 495 (1987).
- [12] I.I. Gontchar, M.V. Chushnyakova, *Comput. Phys. Commun.* **181**, 168 (2010).
- [13] I.J. Thompson, *Comput. Phys. Rep.* **7**, 167 (1988).
- [14] B. Buck, A.A. Pilt, *Nucl. Phys. A* **280**, 133 (1977).